Generalization of the adsorption process in crystalline porous materials and its application to Metal-Organic Frameworks (MOFs)

Jose L. Mendoza-Cortes[1, 2, 3, *] and Alexander A. Aduenko[4]

[1] *Department of Chemical & Biomedical Engineering, FAMU-FSU College of Engineering, Florida State University, Tallahassee FL, 32310, USA*

[2] *Scientific Computing Department, Materials Science and Engineering, High Performance Materials Institute, Florida State University, Tallahassee FL, 32310, USA*

[3] *Condensed Matter Theory, National High Magnetic Field Laboratory, Tallahassee FL, 32310, USA*

[4] *Department of Control and Applied Mathematics, Moscow Institute of Physics and Technology, 9 Institutsky lane, Dolgoprudny, 141700, Russia*

arXiv:1401.2630v3 [cond-mat.mtrl-sci] 18 Sep 2015

In this paper we present an approach for the generalization of adsorption of light gases in crystalline porous materials. Our approach allows the determination of gas uptake considering only geometrical constrains of the porous framework and interaction energy of the guest molecule with the framework. The derivation of this general equation for the uptake of any crystalline porous framework is presented. Based on this theory, we calculated optimal values for the adsorption enthalpy at different temperatures and pressures. We also present the use of this theory to determine the optimal linker length for a topological equivalent framework series. We validate this theoretical approach by comparing the predicted uptake to experimental values for MOF-5, MOF-14, MOF-177, MOF-200, SNU-77H and Li-metalated MOF-177 and MOF-200. We obtained the universal equation for optimal linker length given a topology of a porous framework. This work applies the general equation to Metal-Organic Frameworks (MOFs) but it can be used for other crystalline materials such as Covalent-Organic Frameworks (COFs) and Zeolitic imidazolate frameworks (ZIFs). These results will serve to design new porous materials that exhibit high net storage capacities, in particular for molecular hydrogen (H_2).

I. INTRODUCTION

We present an approach that allows the determination of gas uptake in crystalline porous materials considering only geometrical constraints for the crystal and its interaction energy with the guest molecule. The derivation of this general equation for the uptake of crystalline porous frameworks was validated with experimentally available data for Metal-Organic Frameworks (MOF). We applied this general equation to calculate the net storage capacity of molecular hydrogen storage (H_2) in MOFs. In this work we propose the ideal interaction energy and the ideal linker length for Metal-Organic Frameworks (MOF) given a topology (or crystalline lattice Figure 1), however, in principle, this approach can be extended to any crystalline porous material. Currently there are not simple guidelines for the optimal design of the linker length and the storage capacity of porous frameworks. These results will serve to design materials that maximize net gas storage capacity.

This paper is organized into several sections. In sub-

The derivation of the general formula for the adsorption process is solely restricted to the topology of the framework. We define the topology of a framework as the connectivity in all directions to make a periodic structure. A simple example is shown in Figure 1. This topology is going to determine the number of absorption sites sections IIA and IIB, we derive the general equation for adsorption in any framework, given its geometric properties (i.e. void volume, pore volume, surface area and pore size) and enthalpy of adsorption with the guest molecule (i.e. interaction energy with the surface). We also describe an approach to find the effective number of layers in the more realistic restricted multilayer theory (RMT). Frameworks with several types of topologies (cells) are also considered. In subsection IIIA, we compare our predictions of adsorption isotherm to experimental measurements for system temperatures $T = 77, 243, 273$ and 298 K. In subsection IIIB we derive the optimal enthalpy of adsorption and linker-length/void-volume for the highest net gas storage capacity between atmospheric pressure and the maximum pressure a tank can achieve.

II. METHODOLOGY

A. Restricted multilayer adsorption theory

available for our system.

The first set of theories available to estimate the adsorption properties of surfaces were the Langmuir theory, published in 1916, followed by the Brunauer-Emmett-Teller (BET) theory, published in 1938 [1, 2]. However these two theories, though very useful, have limited application to crystalline porous materials. The Langmuir theory assumes that only one layer of sorbate molecules can be formed on the surface, whereas the BET theory assumes that an infinite number of layers can exist. Both

* jmendozacortes@fsu.edu

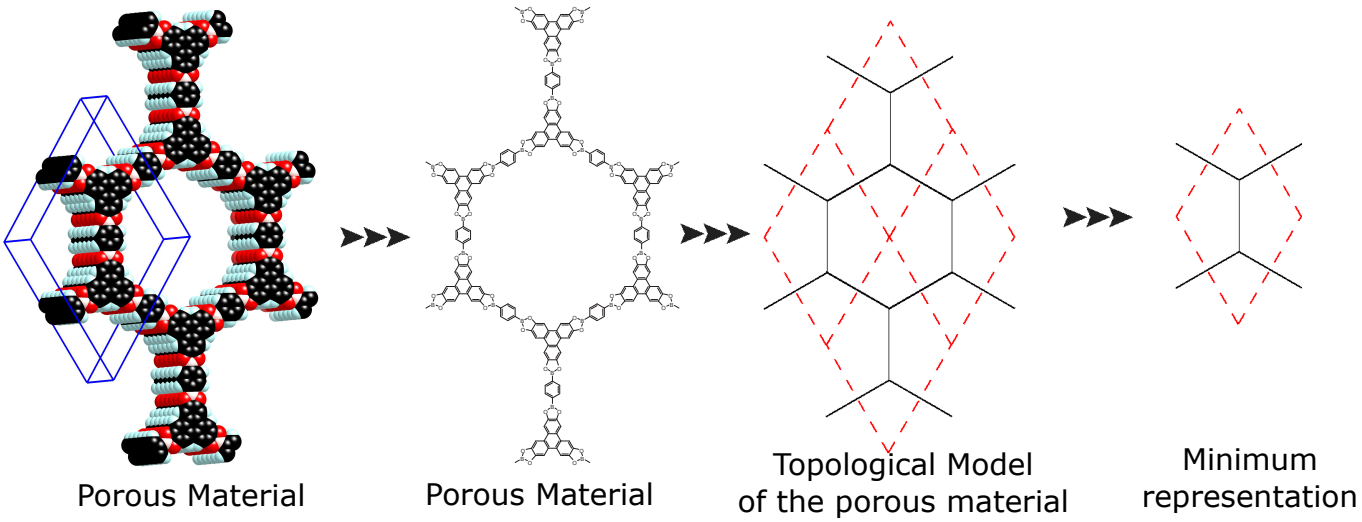

Figure 1: A Porous Framework in converted into a topological construction, i.e. in only edges and nodes

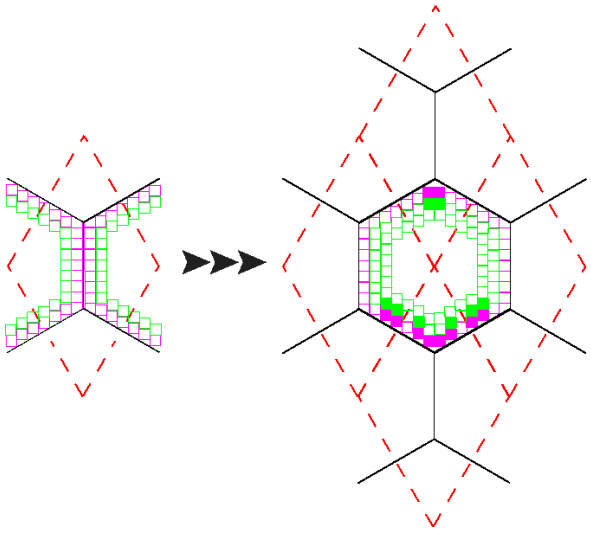

Figure 2: Restricted number of multilayers without (left) and with (right) absorbed gas.

assumption are unphysical for a crystalline porous material, which can usually host more than one layer, but not an infinite number. Thus, a more appropriate approach is needed to treat the case of adsorption in crystalline porous materials, which we call restricted multilayer theory (RMT) in this work. The derivation of the Langmuir and BET theories can be found in the Suplementary Information (Section VI) or elsewhere [1, 2]. We will show below that the equation for a restricted number of multilayers is a more general equation that gives the Langmuir and the BET theory as solutions.

Restricted Multilayer theory (RMT) For the general system presented in Figure 2 we posit that there are B equivalent sites, and N molecules can be distributed in them. We assume that there are only three types of interactions in the system, which are

1. Those between the surface ($n = 0$) and first layer molecules ($n = 1$), with partition function j_1
2. Those between first layer molecules ($n = 1$) and second layer molecules ($n = 2$), with partition function j_2, and
3. Those between n^{th} ($n > 1$) layer molecules and $n^{\text{th}} + 1$ layer molecules, with partition function j_∞.

This creates a columnar structure of bound molecules. Additionally, we assume that there are no interactions between molecules of neighboring columns and the partition function j_2 is equal to j_∞. Given the total number of molecules, N, then N_1 of them are in the first layer and $N_n = N - N_1$ are in higher layers. From these set of assumptions, we can derive the adsorption behavior for a restricted number of multilayers (n layers).

Using the grand canonical partition function, we have

$$\begin{aligned}\Xi(B,\mu,T) &= \sum_{N\geq 0} \exp[(N\mu)/kT]\, Q(N,B,T) \\ &= \sum_{N_1=0}^{B}\sum_{N_2=0}^{N_1}\sum_{N_3=0}^{N_2}\cdots\sum_{N_n=0}^{N_{n-1}} \frac{B!}{(B-N_1)!N_1!} \\ &\quad\times\frac{N_1!}{(N_1-N_2)!N_2!}\cdots \\ &\quad\times\frac{N_{n-1}!(cx)^{N_1}x^{N_2+\ldots+N_n}}{(N_{n-1}-N_n)!N_n!}.\end{aligned}$$

In the preceding equations, μ is chemical potential, T is temperature and k is Boltzmann constant.

Summing in turn over N_n, N_{n-1}, ..., N_1 we find

$$\begin{aligned}\Xi &= [1 + cx(1 + x + x^2 + \ldots + x^{n-1})]^B \\ &= \left[1 + cx\left(\frac{1-x^n}{1-x}\right)\right]^B\end{aligned}$$

where we have defined,

$$c = j_1/j_\infty, \;\; x = j_\infty \exp(\mu/kT).$$

Using this equation in conjunction with the identity,

$$\overline{N} = kT \left(\frac{\partial \log \Xi}{\partial \mu} \right)_{T,B},$$

we find the equation for the *adsorption of a restricted number of multilayers*:

$$\frac{\overline{N}}{B} = \frac{cx[1-(n+1)x^n + nx^{n+1}]}{(1-x)(1-x+cx-cx^{n+1})}. \qquad (1)$$

This equation is more general because the substitution of $n = 1$ or $n = \infty$ gives the Langmuir and BET equations, respectively (Sup. Info. VI). Similar results were obtained earlier [4, 5], however in these treatments, the topology of the framework, along with other geometrical constraints and the specific gas properties were not taken into account. We do this in the following section.

B. General equation for estimation of the molecular uptake for any framework using restricted multilayer theory (RMT)

Here we derive a general equation for the uptake, m, defined as the total mass of gas that can be incorporated per unit volume of porous framework (in units of g/L). This equation applies for any framework based on the RMT of adsorption and the geometric constraints of the framework.

Given that the molar mass of hydrogen $M = 2.018$ g/mol, the uptake per $V = 1\,L = 10^{27}\text{Å}^3$ equals

$$m = M\frac{N}{N_A} = M\frac{\gamma V}{V_p N_A} B \frac{N}{B}(\tilde{n}),$$

where V_p is the volume of a pore, B is the number of sites per pore, N is a number of adsorbed hydrogen molecules per 1 L of adsorbent and N_A is the Avogadro constant. The factor γ corresponds to the fraction of free (or void) volume for the framework, i.e. void volume $= \gamma V$. $\tilde{n}$ is the effective number of layers (Supl. Info. section VIII). We also consider $D+\delta$ as the effective diameter of the absorbed molecule which equals $2r_w = 2 \cdot 2.76$ Å for hydrogen (see Sup. Info.). Using this model it is possible to estimate the number of adsorption sites B as

$$B = \frac{S}{\pi r_w^2},$$

where S is a surface area of one cell.

Strictly speaking we should also consider edge effects when one hydrogen molecule occupies two or more different sites. These considerations will be accounted for elsewhere. However, we should note that edge effects are significant only for nets for which the linker length is nearly the same as the diameter of guest gas molecule. Most known synthesized frameworks have linker lengths that are significantly larger than the hydrogen molecule diameter, thus the edge effects should be negligible for current synthesized materials.

Finally, we obtain the equation for uptake, which can be applied to any type of framework with only one type of conventional unit cell.

$$m = \frac{\gamma \mu V}{N_A \pi r_w^2} \frac{S_p}{V_p} \frac{N}{B}(\tilde{n}). \qquad (2)$$

S_p and V_p in equation (2) are pore surface area and pore volume, respectively.

The occupancy ratio $\dfrac{N}{B}(\tilde{n})$ is defined using the RMT (1) by assuming that j_1 and j_∞ are linked with enthalpies of adsorption on the first ΔH_{ads} layer and higher layers ΔH^*_{ads} as follows (for more details see Supp. Info VI B).

$$j_1 = \exp(\Delta H_{\text{ads}}/RT), \; j_\infty = \exp(\Delta H^*_{\text{ads}}/RT)$$

Let us derive a more general equation for frameworks which have M types of the conventional unit cells with volumes and surface areas V_p^i and S_p^i, respectively. We also introduce factors $\gamma_1, \ldots, \gamma_M$ for the fraction of volume occupied by every type of the cell.

$$\gamma = \sum_{i=1}^{M} \gamma_i.$$

Applying equation (2) to every type of cell separately, we get the total uptake

$$\boxed{m = \sum_{i=1}^{M} \frac{\gamma_i \mu V}{N_A \pi r_w^2} \frac{S_p^i}{V_p^i} \frac{N}{B}(\tilde{n_i}).} \qquad (3)$$

This equation is very general. In fact, it can be used for the challenging problem of predicting the uptake of multivariate Metal-Organic Frameworks (MTV-MOFs) where the pore volume changes due to the different functionalities of its linkers [3], thus generating a supercell of different types of cells where the uptake is not the average, but a more complex relationship. The application of this equation to the different MTV-MOFs is beyond the scope of the current work.

III. RESULTS AND DISCUSSIONS

A. Comparison to experiments.

T =77 K. In order to validate our results, we compared our predictions to experimental data for different MOFs at $T = 77$ K. We took 6 reported frameworks, namely MOF-5, MOF-177, MOF-14, SNU-77H and MOF-200 for this comparison. Data over geometric properties and adsorption enthalpy was taken from published data. We used the restricted multilayer adsorption equation Eq. (3) for the calculations. We present the results we obtained for these framework in Table I. The agreement between experimental and theoretical uptake is within 4 % at this temperature. In Figure 3, we also compared the experimental and theoretical full isotherm at $T = 77$ K for MOF-5 and MOF-177. The agreement is fairly good, however there are some discrepancies in the pressure range of 5-30 bar. This can be explained by the slight decrease of adsorption enthalpy reported in [9], thus suggesting that an effective ΔH_{ads} should be used rather that the one at low coverage as reported in experiments (see Sup. Info. IX).

T=298 K. We also compare our theory with Grand Canonical Monte Carlo (GCMC) simulations for Li-metalated frameworks. Han et al. in [18] considered Li-metalated frameworks with high enthalpy of adsorption at room temperature. This enthalpy decreases significantly with increasing uptake. We took this change in enthalpy into account and defined an effective enthalpy (see Suppl. Info. IX) for every considered pressure. We made an assumption that introducing lithium does not significantly influence the geometric properties of the framework, as suggested in [18], and therefore we used the same geometric parameters of the non-metalated frameworks. The theoretical results for the three different temperatures $T = 243$ K, $T = 273$ K and $T = 298$ K were compared with simulations (see Figure 4). The theoretical predictions are in good agreement with the GCMC results in the entire pressure range. The average absolute deviation for two compounds are reported in table II; this error does not exceed 2.2 %.

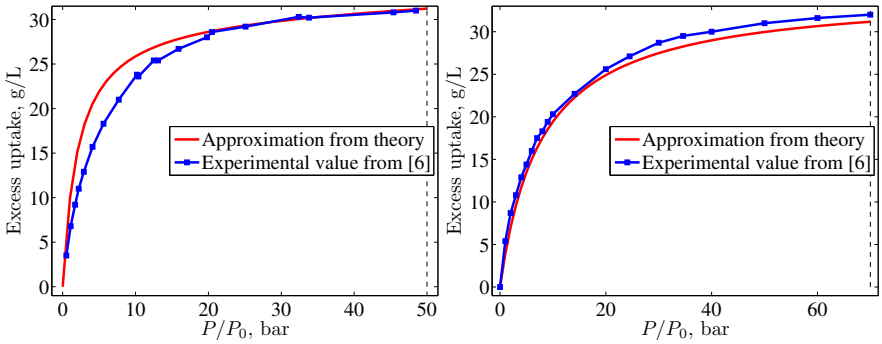

(a) MOF-5, 77 K (b) MOF-177, 77 K

Figure 3: Comparison of theory and experiments for hydrogen isotherm in (a) MOF-5 and (b) MOF-177 at T=77 K.

Table I: Experimental and theoretical *excess* uptake for different MOFs given their geometrical properties. ΔH_{ads} is given as the enthalpy of adsorption, a is the characteristic length of the cell in a framework, and S_A is the surface area.

Compound	a, Å	Void vol., γ	$\tilde{n}$	S_A, m^2/g	V_p, cm^3/g	ΔH_{ads}, kJ/mol	P, bar	Exp., g/L	Theor., g/L	Err.,%
MOF-5	12 [8]	0.798	2	2900 [8]	1.04 [8]	4.8 [16]	50	31.0 [9]	31.22	+0.7
MOF-14	7.7, 14 [12]	0.67 [12]	2	2000 [12]	0.71 [13]	7.0 [13]	40	28.1 [13]	27.25	-3.0
SNU-77H	8 [14]	0.69 [14]	2	3900 [11]	1.52 [11]	7.05 [11]	90	47.4 [11]	49.26	+3.9
MOF-200	18 [8]	0.90 [15]	3	6400 [15]	3.59 [15]	3.46 [17]	90	16.5 [15]	17.18	+4.0
MOF-177	8.5 [9]	0.83 [8]	1	4740 [8]	1.59 [11]	4.4 [9]	70	32.0 [9]	31.17	-2.6

B. Optimal parameters of the framework for the highest gas delivery using the RMT

The ultimate goal of making porous materials for storing hydrogen is not only to store as much molecular hydrogen as possible at some fixed pressure P (usually 100 bar), but also to deliver the maximum amount of hydrogen to the surrounds upon depressurization, which is known as the delivery amount of the storage device. This is defined as the difference in uptake between the atmospheric pressure, P_0 (usually 1 bar), and the maximum

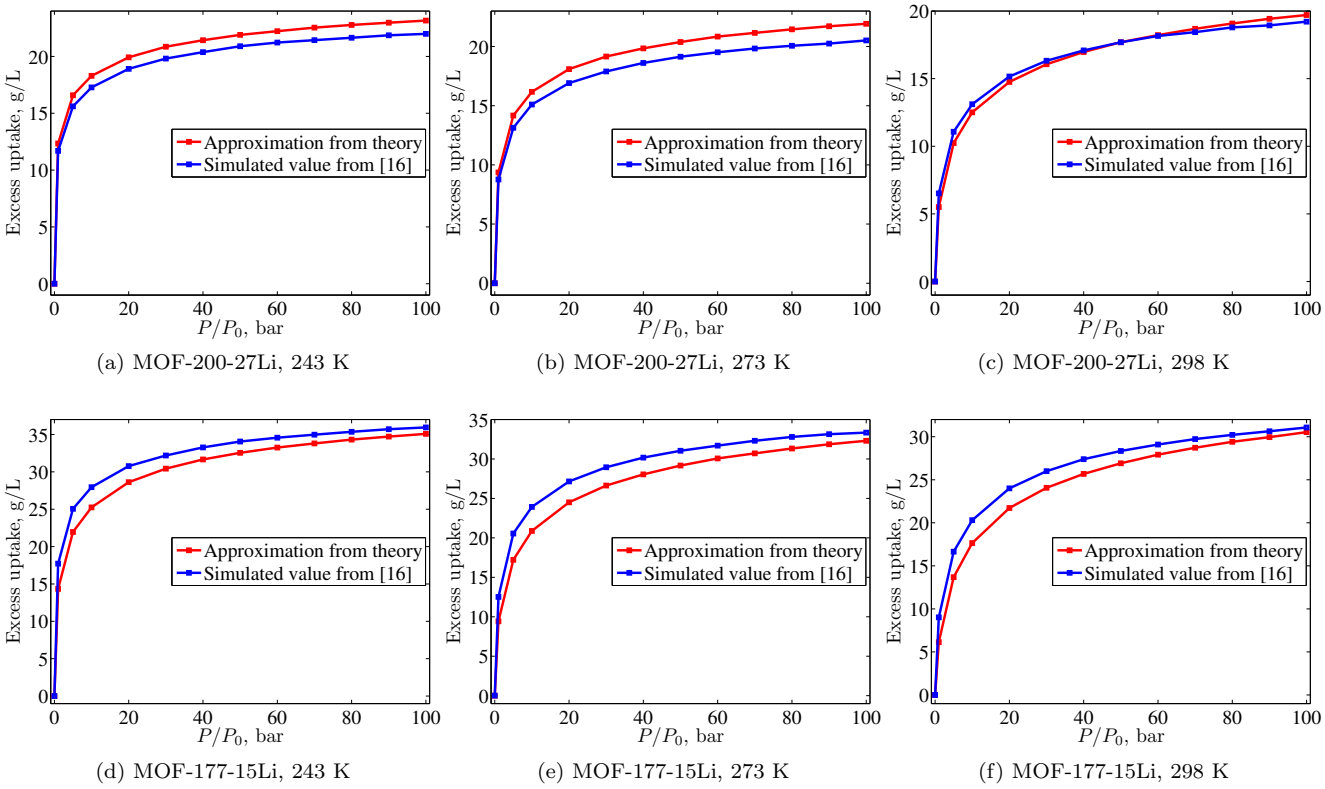

(a) MOF-200-27Li, 243 K (b) MOF-200-27Li, 273 K (c) MOF-200-27Li, 298 K

(d) MOF-177-15Li, 243 K (e) MOF-177-15Li, 273 K (f) MOF-177-15Li, 298 K

Figure 4: Theoretical and simulated adsorption isotherms for (a-c) MOF-200-27Li and (d-f) MOF-177-15Li.

Table II: Average absolute deviation of excess uptake in g/L for MOF-177-15Li and MOF-200-27Li

Compound	$T = 243$ K	$T = 273$ K	$T = 298$ K
MOF-177-15Li	1.80 (6.0%)	2.12 (7.1%)	1.67 (5.6%)
MOF-200-27Li	1.02 (5.0%)	1.21 (6.0%)	0.40 (2.0%)

pressure of the tank, P (typically 100 bar). Therefore, obtaining the maximum delivery amount is the most important characteristic of a storage device. We propose doing this by obtaining an optimal enthalpy of adsorption ΔH_{ads}^{opt}. Porous materials with low ΔH_{ads} do not store enough gas, even at the maximum pressure P. On the other hand, if ΔH_{ads} is too high the framework retains all the adsorbed gas at low pressure, and the gas cannot be used either. In both cases, the delivery amount is negligible.

We first derive equations for optimal enthalpy of adsorption, ΔH_{ads}^{opt}, using RMT. Then, we present an approach of determining the optimal geometric properties (i.e. effective linker length) for a given series of frameworks.

Enthalpy of adsorption ΔH_{ads}. First, we find optimal values of ΔH_{ads} in a low-temperature region (for instance, for $T = 77$ K), where rotational degrees of freedom are not significantly activated. Nevertheless this theory is further applied for high temperatures (for instance, for $T = 298$ K), just by considering the full chemical potential (Supl. Info. XI). One may use the full chemical potential for the low temperature region as well. However in this region the equilibrium ratio of para- and ortho- hydrogen is far from 3:1. This implies full quantum mechanical considerations of ortho and para- hydrogen without simplification (see Suppl. Info. XI, XII). However this does not change the result significantly because the rotational degrees of freedom are not activated at low temperature.

According to our theory, geometric properties of a framework only define some factors to the uptake. The shape of the isotherm is defined by the factor $\nu = N/B(\tilde{n})$ from the RMT. Thus to get the highest delivery amount for fixed number of layers (fixed geometry) one must derive the enthalpy ΔH_{ads} that leads to the highest possible difference in the factor ν between pressure P_0 and P.

$$\Delta\nu = [\nu(P) - \nu(P_0)] \to \max_{\Delta H_{ads}} .$$

The function $\nu(P)$ is smooth, thus the necessary condition to obtain the maximum is

$$\frac{\partial \Delta\nu}{\partial \Delta H_{ads}} \left(\Delta H_{ads}^{opt}\right) = 0. \qquad (4)$$

For convenience we introduce the multiplier m defined as $P = m\,P_0$

We also define

$$\beta_1 = \exp\{\Delta H_{ads}/(RT)\},\ \beta_2 = \exp\{\Delta H^*_{ads}/(RT)\},$$

$$\tilde{\beta_1} = \alpha\beta_1,\ \tilde{\beta_2} = \alpha\beta_2,$$

$$c = \beta_1/\beta_2,\ x = \alpha P/P_0\beta_2.$$

Here, H^*_{ads} is the interaction of first layer with the second layer of adsorbed molecules.

$$\alpha = \frac{P_0}{P}\exp(\mu/kT)$$

is a function of temperature. For the low temperature region chemical potential is defined by a translational part ($\mu \approx \mu_{tr}$) and

$$\alpha = \frac{P_0}{kT}\left(\frac{\mu kT}{2\pi N_A\hbar^2}\right)^{-3/2}.$$

For the high temperature region, when rotational degrees of freedom are fully activated

$$\alpha = \frac{P_0}{kT}\left(\frac{\mu kT}{2\pi N_A\hbar^2}\right)^{-3/2}\left(\frac{2T_r}{T}\right). \quad (5)$$

Here μ is molar mass of gas, T_r is the activation temperature for rotational degrees of freedom, and $P_0 = 1$ bar.

Deriving $\partial\Delta\nu/\partial\Delta H_{ads}$ for the RMT gives the values for optimal enthalpy ΔH^{opt}_{ads}. Thus, the optimal enthalpy for the **restricted multilayer case** is given by eq. (6).

$$\Delta H^{opt}_{ads} = RT\ln\beta_1 = RT\ln\tilde{\beta}_1/\alpha, \quad (6)$$

where

$$\tilde{\beta}_1 = \frac{a(1-m\tilde{\beta}_2) - b\sqrt{m}(1-\tilde{\beta}_2)}{b\sqrt{m}(1-\tilde{\beta}_2^n) - am(1-m^n\tilde{\beta}_2^n)},$$

$$a = \sqrt{1-(n+1)\tilde{\beta}_2^n + n\tilde{\beta}_2^{n+1}},$$

This table shows the similar performance for different amount of layers. Thus figures are the same for RMT for any number of layers. In other words, the plots for $n = 2, 3, 6$ look similar and we only show $n = 3$. Discrepancies are noticeable only at very low temperatures and with very different number of layers. From (Eq. 6) we find that the optimal enthalpy increases with temperature.

Finally, we plot the results for the optimized value for $\Delta\nu = \Delta(N/B)$ which directly influences the (see Figure 6). These results show that the difference between all three cases becomes significant only at low temperature. However, one must be cautious for other gases, which have higher ΔH^*_{ads} than hydrogen and this difference can be much more significant when applying the different theories. The safe way, of course, is to use the RMT.

$$b = \sqrt{1-(n+1)m^n\tilde{\beta}_2^n + nm^{n+1}\tilde{\beta}_2^{n+1}}.$$

Particularly for the high-temperature region, (e.g. T=298 K), and the associated value of α (5) we get

$$\Delta H^{opt}_{ads} = RT\ln\beta_1 = RT\ln\left(\tilde{\beta}_1 T^{7/2}/\left(\alpha_0 T_0^{7/2}\right)\right), \quad (7)$$

where $\alpha_0 = 5.1\cdot 10^{-6}$, $T_0 = 298$ K and

$$\tilde{\beta}_1 = \alpha_0\,(T_0/T)^{7/2}\,\beta_1.$$

Thus for the RMT, for example at $T_0 = 77$ K, $P = 100$ bar, $n = 3$, we have $\Delta H^{opt}_{ads} = 3.81$ kJ/mol. On the other hand, at $T_0 = 298$ K, $P = 100$ bar, $n = 3$, we have $\Delta H^{opt}_{ads} = 24.5$ kJ/mol.

The optimal $\Delta\nu$ is defined as $\nu(P) - \nu(P_0)$ where $\tilde{\beta}_1$ is denoted optimal given by Eq. 7. The optimal $\Delta\nu$ for $n = 1$ or the Langmuir case can be obtained if $\tilde{\beta}_2 = 0$ and therefore $a = b = 1$ in the previous equations. Similarly, the optimal $\Delta\nu$ for $n = \infty$ or the BET case can be derived by excluding powers of $\tilde{\beta}_2$ higher than first power and setting therefore $a = b = 1$. This is another example where the restricted multilayer theory is the general case for the Langmuir and BET theories.

Now, to illustrate the consequences of these equations we first plot optimal enthalpy at different temperatures and different number of layers ($n = 2, 3, 6$) in Figure 5 and show some of the values in table III.

Table III: Optimal enthalpy $\Delta H^*_{\rm ads}$ for different temperature T and number of layers n for $P = 100$ bar

Number of layers n	$T = 50$ K	$T = 77$ K	$T = 298$ K
1	2.02	3.80	24.48
2	1.99	3.80	24.48
3	1.99	3.81	24.48
6	1.99	3.81	24.48

Optimal length of the linker and void volume. In the previous section we obtained the optimal value of enthalpy which influences the shape of the isotherm. Here, we present an approach to define optimal linker length for a series of frameworks. The linker length does not influence the shape of the curve, but it does influence its asymptotic value (when $P \to \infty$). This is because the pore volume V_p, surface area S_p and fraction of void volume γ depend on the linker length.

To get the optimal linker length we consider the general

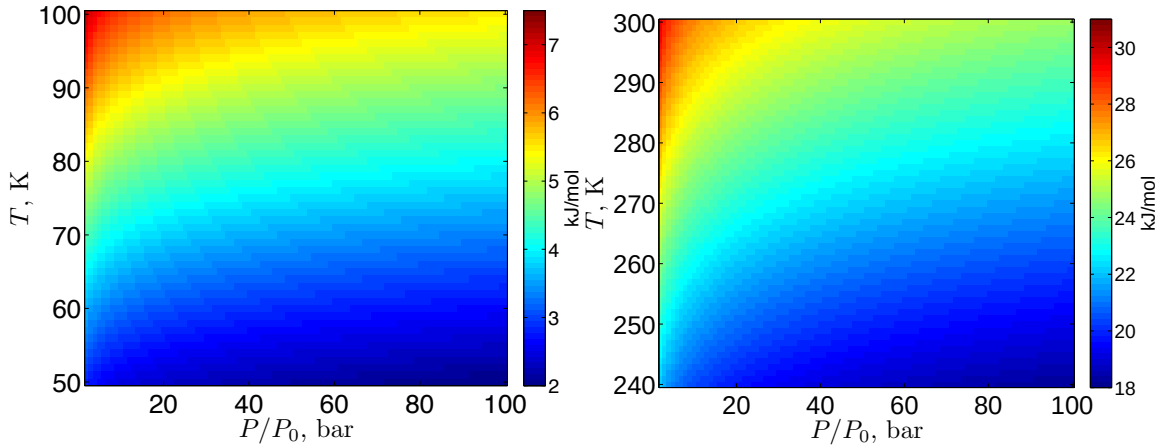

(a) Restricted multilayer case, 50-100 K, $n = 3$

(b) Restricted multilayer case, 240-300 K, $n = 3$

Figure 5: Temperature and pressure dependence of optimal enthalpy ΔH_{ads}^{opt} for low and high temperature region and n=3.

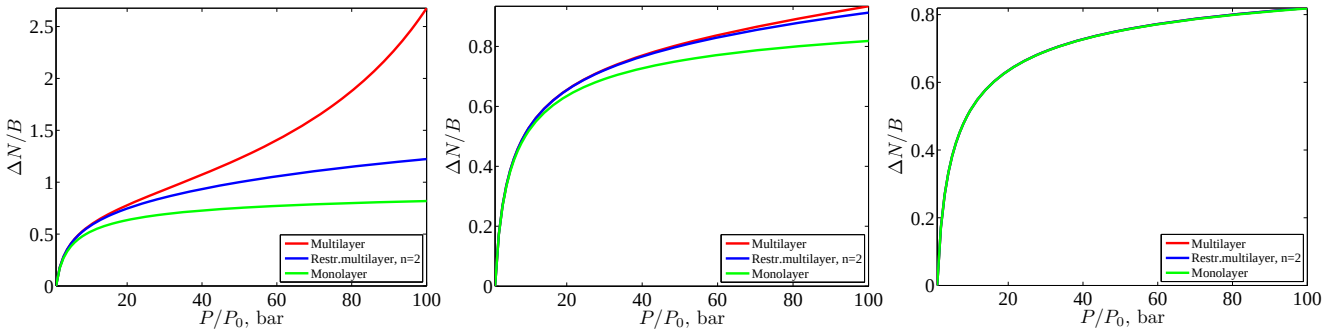

(a) T=50 K

(b) T=77 K

(c) T=298 K

Figure 6: $\Delta\dfrac{N}{B}$ for different temperatures

equation for uptake one more time (Eq. 3) and, using one type of cell ($M = 1$), we obtain (Eq. 2),

$$m = \frac{\gamma\mu V}{N_A \pi r_w^2} \frac{S_p}{V_p} \frac{N}{B}(\tilde{n}).$$

The factor $(N/B)(\tilde{n})$ has been considered in the previous section. Now we consider the second one

$$\gamma \frac{S_p}{V_p}$$

since all the other terms are constant and do not depend on the geometrical characteristics of the framework. We assume that the framework has one characteristic length a, which is the length of the linker. We assume that the net can be expanded based on a reduced unit cell. Total volume is given as $V \sim a^3$, but for the volume of the framework itself we suggest $V_{net} \sim a^{1+\xi}$, where ξ indicates how the volume of the net grows with the growth of a. For instance, if $\xi = 0$, it means that the volume of the net grows only with linker length, whereas the cross section of linkers is constant.

Thus we get

$$\gamma = 1 - \frac{V_{net}}{V} = 1 - \frac{\kappa}{a^{2-\xi}}, \tag{8}$$

where κ is some constant depending on the framework. We also get $S_p/V_p = c/a$, where c is constant for every framework not changing when enlarging the linkers. Thus,

$$f(a) = \gamma \frac{S_p}{V_p} = \left(1 - \frac{\kappa}{a^{2-\xi}}\right) \frac{c}{a} \to \max_a .$$

This gives

$$a^{2-\xi} = (3 - \xi)\kappa$$

and therefore

$$a = ((3-\xi)\kappa)^{\frac{1}{2-\xi}}. \tag{9}$$

The factor κ can be easily defined from experimental data if γ is known for at least one length of the linker a or can be measured directly for any framework just by using geometry. Therefore, we obtain the universal recipe of best linker length under these assumptions.

To show an example, given $\xi = 0$, for any framework the best value is

$$\gamma = 1 - \frac{\kappa}{(\sqrt{3\kappa})^2} = 2/3.$$

Now we apply equation (9) to the topologically equivalent IR-MOFs, IRMOF-1 to IRMOF-16. This will determine the optimal length of the linker for such frameworks and therefore the optimal void volume. First we determine the model parameters κ and ξ. To get this we several calculations that follow. Rearranging Eq. 8 we obtain

$$\log(1-\gamma) = \log\kappa - (2-\xi)\log a.$$

Now, using the data over the fraction of void volume γ and the effective linker length V_p/S_p for the considered IRMOFs, we obtain ξ and κ using a linear regression (Figure 7a). The regression has a high correlation coefficient, $R^2 = 0.9524$ showing the significance of the dependence of the void volume and the effective linker length. Thus for this family of MOFs, we obtain $\log\kappa = -0.015$, $2-\xi = 0.932$ and the estimations for the coefficients are $\kappa = 0.966$, $\xi = 1.068$.

Thus we get the optimal void volume $\gamma = 0.4824$. and the optimal effective linker length $(V_p/S_p) = 1.95\mathring{A}$. Note that the effective linker length is not the same as the linker length alone. For instance, for a cubic cell, the effective linker length is $a^3/(6a^2)$ which is 6 times smaller than the linker length a. The closest one to the reported figures is IRMOF-5 with $\gamma = 0.5$ and $a = 2.05$ Å, which correspond to 98.5% of the predicted optimal uptake for this framework.

The optimal quantity for effective linker length is close to the value for IRMOF-5 and therefore further improvements for the IRMOFs should not consider the linker length but instead the enthalpy of adsorption (24.5 kJ/mol, for $n = 1$ and $T = 297$ K, given that not more than one layer of hydrogen can be inserted in such pores).

IV. CONCLUSIONS

We presented a theory for a realistic restricted multilayer adsorption of gases in crystalline porous materials. We applied this theory to estimate molecular hydrogen adsorption in Metal-Organic Frameworks (MOFs) and our approximations predict uptakes that agree with experimental values at 77 K and 298 K. We found that the results for this theory can differ from the Langmuir and BET theories at low temperatures.

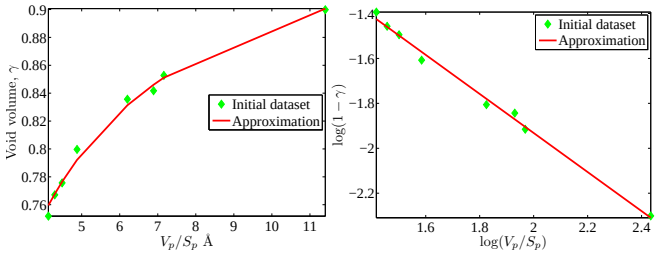

(a) Fit in normal axes (b) Linear fit in logarithmic scale

Figure 7: Void volume dependence on linker length. Notice the logarithmic axes in (b) and its direct correlation

For compounds that are isoreticular to MOF-5 (topology **pcu**), we found that the optimal effective linker length is 1.95 Å and the enthalpy of adsorption is 3.75 kJ/mol at 77 K and 24.5 kJ/mol at 298 K, respectively, which will give a maximum expected delivery amount of 81.8% or 34.65 g/L.

V. SUPPORTING INFORMATION.

Full derivations for normal non-interpenetrated and interpenetrated frameworks, low and high temperature considerations, analyses of different multilayers and enthalpies of the adsorption, and other comparisons to experiments. This material is available free of charge on the Internet at http://pubs.acs.org/.

[1] Langmuir, I. The Constitution and Fundamental Properties of Solids and Liquids. Part I. Solids. *J. Am. Chem. Soc.* **1916**, *38*, 22212295.

[2] Brunauer, S. ;Emmett P. H.; Teller, F. Adsorption of Gases in Multimolecular Layers *J. Am. Chem. Soc.* **1938**, *60*, 309-319.

[3] Deng, H.; Doonan, C. J.; Furukawa, H.; Ferreira, R. B.; Towne, J.; Knobler, C. B.; Wang, B.; Yaghi, O. M. Multiple functional groups of varying ratios in metal-organic frameworks. *Science*, **2010**, *327*, 846-850

[4] Hill, T. L. Statistical Mechanics of Multimolecular Adsorption. I *J. Chem . Phys.* **1946**, 14, 263-267.

[5] Keii, T. A Statistical Derivation of the B.E.T. Equation *J. Chem . Phys.* **1954**, *22*, 1617-1618.

[6] Bhatia, S. K.; Myers, A. L. Optimum Conditions for Adsorptive Storage *Langmuir* **2006**, *22*, 1688-1700.

[7] M. W. Chase Jr., NIST-JANAF Thermochemical Tables, 4th Edition *J. Phys. Chem. Ref. Data*, Monograph(9) **1998**, 1-1951.

[8] M. Eddaoudi et al. Eddaoudi, M.; Moler, D.B, Li, H.; Chen, B.; Reineke, T.M.; O'Keeffe, M.; Yaghi O.M. Modular chemistry: secondary building units as a basis for the design of highly porous and robust metal-organic carboxylate frameworks. *Accounts of Chemical Research* **2001**, *34*, 319-330.

[9] Wong-Foy, A. G.; Matzger, A. J.; Yaghi, O. M.; Exceptional H2 saturation uptake in microporous metal-organic frameworks. *J. Am. Chem. Soc.* **2006**, *128*, 3494-3495.

[10] Kaye, S. S.; Dailly, A.; Yaghi, O.M.; Long, J.R. Impact of preparation and handling on the hydrogen storage properties of Zn4O(1,4-benzenedicarboxylate)3 (MOF-5). *J. Am. Chem. Soc.* **2007**, *129*, 14176-14178.

[11] Suh, M.P.; Park, H.J.; Prasad T.K.; Lim, D.W. Hydrogen storage in metal-organic frameworks. *Chem. Rev.* **2012**, *112*, 782-835.

[12] Chen, B.; Eddaoudi, M.; Hyde, S. T.; O'Keeffe, M.; Yaghi1, O. M. Interwoven Metal-Organic Framework on a Periodic Minimal Surface with Extra-Large Pores. *Science* **2001**, *291*, 1021-1023.

[13] O. M. Yaghi, Hydrogen Storage in Metal-Organic Frameworks, **2008**. URL: http://books.quality3.org/h/hydrogen-storage-in-metal-organic-frameworks-book-w7531/

[14] Park, H.J.; Lim, D.-W.; Yang, W. S.; Oh, T.R.; Suh, M.P. A Highly Porous MetalOrganic Framework: Structural Transformations of a Guest-Free MOF Depending on Activation Method and Temperature *Chem. - Eur. J.* **2011**, *17*, 7251-7260.

[15] Furukawa, H.; Ko, N.; Go, Y.B.; Aratani, N.; Choi, S.B.; Choi, E.; Yazaydin, A.O.; Snurr, R.Q.; O'Keeffe, M.; Kim, J.; Yaghi, O.M. Ultrahigh porosity in metal-organic frameworks. *Science* **2010**, *329*, 424-428.

[16] Rowsell,J. L.; Yaghi,O. M. Effects of functionalization, catenation, and variation of the metal oxide and organic linking units on the low-pressure hydrogen adsorption properties of metal-organic frameworks. *J. Am. Chem. Soc.* **2006**, *128*, 1304-1315.

[17] Mendoza-Cortes, J. L.; Han, S.S.; Goddard, W. A. High H2 uptake in Li-, Na-, K-metalated covalent organic frameworks and metal organic frameworks at 298 K. *J. Phys. Chem. A* **2012**, *116*, 1621-1631.

[18] Han, S.S.; Jung, D.H.; Choi, S.-H.; Heo, J. Lithium-Functionalized MetalOrganic Frameworks that Show > 10 wt% H2 Uptake at Ambient Temperature *ChemPhysChem* **2013**, *14*, 2698-2703.

[19] L. D. Landau and E. M. Lifshitz, *Statistical Physics* (Butterworth-Heinemann), **1980**, *5*.

Table of Contents

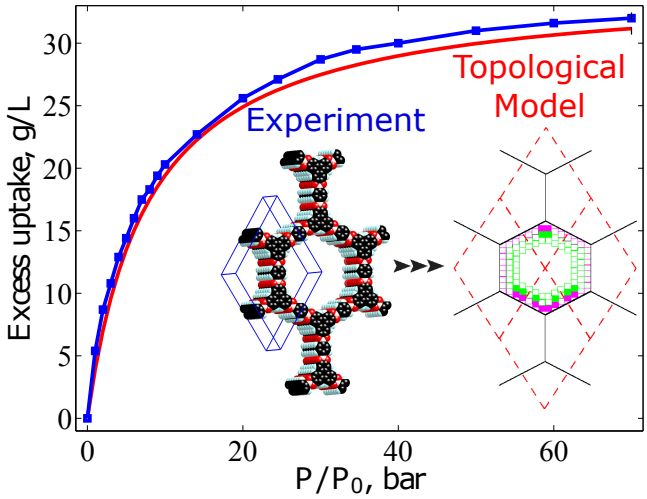

Supporting Information

Generalization of the adsorption process in crystalline porous materials and its application to Metal-Organic Frameworks (MOFs)

Jose L. Mendoza-Cortés[1,2,*], and Alexander A. Aduenko[3]

[1] Department of Chemical & Biomedical Engineering, FAMU-FSU College of Engineering, Florida State University, Tallahassee FL, 32310, USA
[2] Scientific Computing Department, Materials Science and Engineering, High Performance Materials Institute, Condensed Matter Science, National High Magnetic Field Laboratory, Florida State University, Tallahassee FL, 32310, USA
[3]Department of Control and Applied Mathematics, Moscow Institute of Physics and Technology, 9 Institutsky lane, Dolgoprudny, 141700, Russia

E-mail: jmendozacortes@fsu.edu

VI. ADSORPTION THEORY

In this subsection we firstly derive the Langmuir or monolayer theory of adsorption. Following this, we consider Brunauer-Emmett-Teller (BET) or multilayer theory. Finally, we derive a more general RMT. Langmuir and BET theories are its special cases, when the number of adsorption layers equals 1 and ∞ respectively. Finally, we will see that we are able to overcome the unphysical restrictions imposed by Langmuir and BET theories, i.e. the requirement of a monolayer for the the Langmuir theory and for infinite layers for the BET case.

We make the following definition and assumptions based on the postulates above. In the system, there are B equivalent sites, there are N molecules distributed in B sites, there are no interactions between molecules and the lattice may be one-, two-,three-periodic.

A. Derivations of the different sorption theories

Monolayer theory. Using the the Gibbs ensemble (also known as Grand Canonical distribution), we have

$$\Xi(\mu,\tau) = \sum_{N=0}^{\infty}\sum_{S(N)} \exp[(N\mu - \epsilon_{S(N)})/\tau] = \sum_{[S(N),N]} \exp[(N\mu - \epsilon_{S(N)})/\tau],$$

where,

- $[S(N), N]$ is for all states of the system for all number of particles
- $\epsilon_{S(N)}$ defines that each ϵ_S depends on the number of particles. $\epsilon_{S(N)}$ is the energy of the state $S(N)$ of the exact N-particle Hamiltonian.

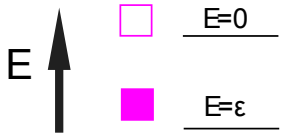

Figure 8: Assumption from Langmuir theory

Now we can calculate the thermal average number of particles by

$$\langle N\rangle = \frac{\sum_{S,N} N\exp[(N\mu - \epsilon_{S(N)})/\tau]}{\Xi}.$$

Combining that with

$$\frac{\partial\Xi}{\partial\mu} = \frac{1}{\tau}\sum_{S,N} N\exp[(N\mu - \epsilon_{S(N)})/\tau]$$

we obtain:

$$\langle N\rangle = \frac{\tau}{\Xi}\frac{\partial\Xi}{\partial\mu} = \tau\frac{\partial\log\Xi}{\partial\mu}.$$

Here we considered only one adsorption site. Let B be the number of adsorption sites. From the definition of

$\lambda = \exp(\mu/\tau)$, we have

$$\frac{\langle N\rangle}{B} = \lambda \frac{\partial \log \Xi}{\partial \lambda} \tag{10}$$

Now we take into account the assumption from the Langmuir theory as two energy states for each particle, as shown in the figure 8. We consider adsorption as favorable process. Therefore, the lower energy corresponds to the adsorbed state, and thus $\epsilon < 0$. Given this, we can derive the partition function as

$$\Xi = 1 + \lambda \exp\left(\frac{-\epsilon}{\tau}\right)$$

Substituting this result into eq. (10), we have

$$\frac{\langle N\rangle}{B} = \frac{\lambda \exp(-\epsilon/\tau)}{1 + \lambda \exp(-\epsilon/\tau)}$$
$$\frac{\langle N\rangle}{B} = \frac{1}{\lambda^{-1} \exp(\epsilon/\tau) + 1}$$

Multilayer theory. It is postulated that a gas molecule can be absorbed on each site B, with partition function j_1, which is denoted as the "first layer". This first molecule can then be used as a site for another "second layer" molecule, and so on. The partition function for the second and subsequent molecules is given as j_∞. If given N total number of molecules, of which N_1 are in the first layer, then $N^* = N - N_1$ are in higher layers (more details can be found elsewhere [4], [5]).

Using the grand canonical partition function, we have

$$\begin{aligned}\Xi(B,\mu,T) &= \sum_{N\geq 0} \exp[(N\mu)/k\tau] Q(N,B,T) \\ &= 1 + \sum_{N_1=1}^{B} \frac{B!(j_1 \exp(\mu/(kT)))^{N_1}}{N_1!(B-N_1)!(N_1-1)!} \\ &\quad \times \sum_{N^*=0}^{\infty} \frac{(N_1+N^*-1)!(j_\infty \exp(\mu/(kT)))^{N^*}}{N^*!}\end{aligned}$$

Furthermore,

$$\Xi(B,\mu,T) = \sum_{N_1=0}^{B} \frac{B!(y)^{N_1}}{N_1!(B-N_1)!} = (1+y)^B \tag{11}$$

where we have defined,

$$y = \frac{j_1 \exp(\mu/kT)}{1 - j_\infty \exp(\mu/kT)}$$

Again using

$$\overline{N} = kT \left(\frac{\partial \log \Xi}{\partial \mu}\right)_{T,B} \tag{12}$$

and applying it to equation 11, we have

$$\frac{\overline{N}}{B} = \frac{cx}{(1-x+cx)(1-x)} \tag{13}$$

where $c = \frac{j_1}{j_\infty}$ and $x = j_\infty \exp(\mu/kT)$. This is also known as the BET adsorption isotherm equation [2].

Restricted Multilayer theory (RMT) A more realistic approach is that the adsorption is restricted to n layers,

$$\begin{aligned}\Xi(B,\mu,T) &= \sum_{N_1=0}^{B} \sum_{N_2=0}^{N_1} \sum_{N_3=0}^{N_2} \cdots \sum_{N_n=0}^{N_{n-1}} \frac{B!}{(B-N_1)!N_1!} \\ &\quad \times \frac{N_1!}{(N_1-N_2)!N_2!} \cdots \\ &\quad \times \frac{N_{n-1}!(cx)^{N_1} x^{N_2+\ldots+N_n}}{(N_{n-1}-N_n)!N_n!}\end{aligned}$$

Summing in turn over N_n, N_{n-1}, ..., N_1, we find,

$$\begin{aligned}\Xi &= [1 + cx(1 + x + x^2 + \ldots + x^{n-1})]^B \\ &= \left[1 + cx\left(\frac{1-x^n}{1-x}\right)\right]^B\end{aligned}$$

Substituting this into equation 12, we find the BET equation for *restricted adsorption*

$$\frac{\overline{N}}{B} = \frac{cx[1-(n+1)x^n + nx^{n+1}]}{(1-x)(1-x+cx-cx^{n+1})} \tag{14}$$

This equation is more general, since assumptions on the number of layers $n = 1$ or $n = \infty$ give the Langmuir and BET equations, respectively. The substitution,

$$\frac{\overline{N}}{B} \xrightarrow{n=\infty} \frac{cx}{(1-x+cx)(1-x)}$$

gives the BET equation, and

$$\frac{\overline{N}}{B} \xrightarrow{n=1} \frac{j_1 \exp(\mu/kT)}{1 + j_1 \exp(\mu/kT)}$$

gives the Langmuir equation.

B. Applications of these formulas to H_2 in porous materials

In this subsection we assume ideal behavior for molecular hydrogen gas and consider no interaction between its molecules. Moreover, we neglect rotations. Consideration of rotations will be reported in subsection VI C. Changes in chemical potential, μ, arising from rotations are fully derived in Suppl. info. Nevertheless, we should

note that for $T = 77$ K rotations are not very significant, as the rotational activation temperature is 85.4 K for hydrogen. Moreover, in order to consider rotations at such a temperature, one must separately consider orthohydrogen and parahydrogen because, at this temperature, their rotational partition functions differ significantly. Thus in this section we consider only translational part of entropy and free energy, which is exact for monoatomic gases, and is quite a good approximation for hydrogen at such a low temperature. In order to obtain consistent results for room temperature, we consider rotations in subsection VI C. There is no issue with orthohydrogen and parahydrogen for room temperature as partition functions for both of them differ only slightly.

In this subsection we firstly apply our assumptions to the Langmuir or monolayer theory of adsorption. Following that, we consider the BET or multilayer theory. Finally, we derive a more general RMT. Langmuir and BET theories are special cases of the RMT, when the number of adsorption layers equals 1 and ∞, respectively.

According to the prior assumptions, we get

$$\lambda = \frac{n}{n_q} = \frac{p}{\tau n_q} = \frac{p}{k_B T n_q}$$

and

$$n_q = \left(\frac{M\tau}{2\pi\hbar^2}\right)^{3/2} = \left(\frac{Mk_BT}{2\pi\hbar^2}\right)^{3/2}$$

Monolayer theory in H_2. If we apply these assumptions to equation 11 we get the Langmuir equation for H_2

$$\begin{aligned}\frac{\langle N\rangle}{B} &= \frac{1}{(n_q\tau/p)\exp(\epsilon/\tau)+1}\\ \frac{\langle N\rangle}{B} &= \frac{p}{(n_q\tau)\exp(\epsilon/\tau)+p}\\ &= \frac{p/p_0}{(n_q\tau)\exp(\epsilon/\tau)/p_0+p/p_0}\end{aligned} \tag{15}$$

where $p_0 = 1$ bar.

Multilayer theory in molecular hydrogen. In order to obtain j_1 and j_∞, the procedure illustrated in Figure 9 was used. We consider adsorption as a favorable process and therefore the energies ϵ_1 and ϵ_∞ are negative relative to the energy of a free molecule. Figure 9 illustrates the common situation when adsorption on higher levels is less favorable than adsorption on the first one and therefore $\epsilon_\infty > \epsilon_1$.

Thus for partition functions j_1 and j_∞, for molecules adsorbed on first and higher levels, respectively, we get

$$\begin{aligned}j_1 &= e^{-\epsilon_1/kT} = e^{\Delta H_{ads}/RT}\\ j_2 &= e^{-\epsilon_{infty}/kT} = e^{\Delta H^*_{ads}/RT}\end{aligned}$$

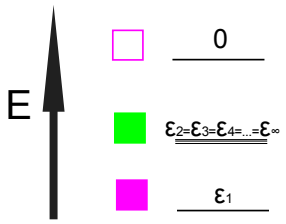

Figure 9: Assumption for the multilayer theory

$$\begin{aligned}\Delta H_{ads}/RT &= \text{Surface}\cdots\text{H}_2\\ \Delta H^*_{ads}/RT &= \quad\text{H}_2\cdots\text{H}_2\end{aligned}$$

Figure 10 illustrates the adsorption process. Filled squares represent adsorbed molecules, and empty squares represent free sites. First layer molecules (colored in magenta) are bonding sites for higher level molecules (colored in green).

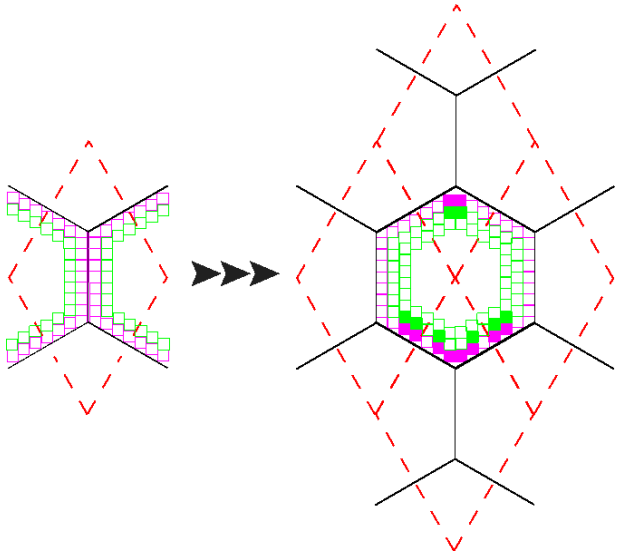

Figure 10: Assumption for the multilayer theory

If we set $\epsilon_2 = 0$, then we will nearly have the case of monolayer theory. There will be some effect due to the existence of higher levels, but it will not be significant in the studied range of pressure (0 to 100 bar). Consider

$$\alpha = \frac{P_0}{kT}\left(\frac{MkT}{2\pi\hbar^2}\right)^{-3/2},$$

where $P_0 = 1$ bar. For $T = 77$ K, $\alpha \approx 2.6 \cdot 10^{-4}$ which is

a relatively small value. In the multilayer case for H_2

$$\frac{\langle N\rangle}{B} = \frac{\alpha\frac{P}{P_0}e^{\Delta H_{ads}/RT}}{1+\left(e^{\Delta H_{ads}/RT}-e^{\Delta H^*_{ads}/RT}\right)\alpha\frac{P}{P_0}}\times \frac{1}{1-\alpha\frac{P}{P_0}e^{\Delta H^*_{ads}/RT}}, \quad (16)$$

where $R = kN_A = 8.314\,\mathrm{J/(mol\times K)}$. For hydrogen,

$$x = \alpha\frac{P}{P_0}\exp\left(\frac{\epsilon_2}{k_BT}\right),$$

and

$$c = \exp\left(\frac{\epsilon_1-\epsilon_2}{k_BT}\right).$$

If we set $\Delta H^*_{ads} = 0$, then for the considered pressures

$$1 \geq 1-\alpha\frac{P}{P_0}e^{\Delta H^*_{ads}/RT} \geq 1-2.6\cdot10^{-4}\times100 \approx 1.$$

If $e^{\Delta H_{ads}/RT} \gg 1$, then

$$\frac{\langle N\rangle}{B} \approx \frac{1}{1+\frac{1}{\alpha}\frac{P_0}{P}e^{-\Delta H_{ads}/RT}},$$

which is exactly the same as equation (15). When increasing ΔH^*_{ads}, the effect from higher layers becomes more noticeable (compare Figure 11a and Figure 11b). Due to the limitation arising from $1-x>0$ in eq. (13), we get

$$\frac{\Delta H^*_{ads}}{RT} < -\log\left[\alpha\frac{P}{P_0}\right].$$

ΔH^*_{ads} is treated as equal to the heat of hydrogen liquefaction and therefore equals 0.904 kJ/mol.

Plotting the isotherm for the hydrogen molecule in the multilayer case for calculated ΔH^*_{ads} for $T = 77$ K (see Figure 11c). However, if ΔH^*_{ads} changes, the shape of the isotherm changes. For example, $\Delta H^*_{ads} = 0$ gives a similar plot to Figure 11c while $\Delta H^*_{ads} = 2\,\mathrm{kJ/mol}$ is very different (see Figure 11b vs Figure 11c).

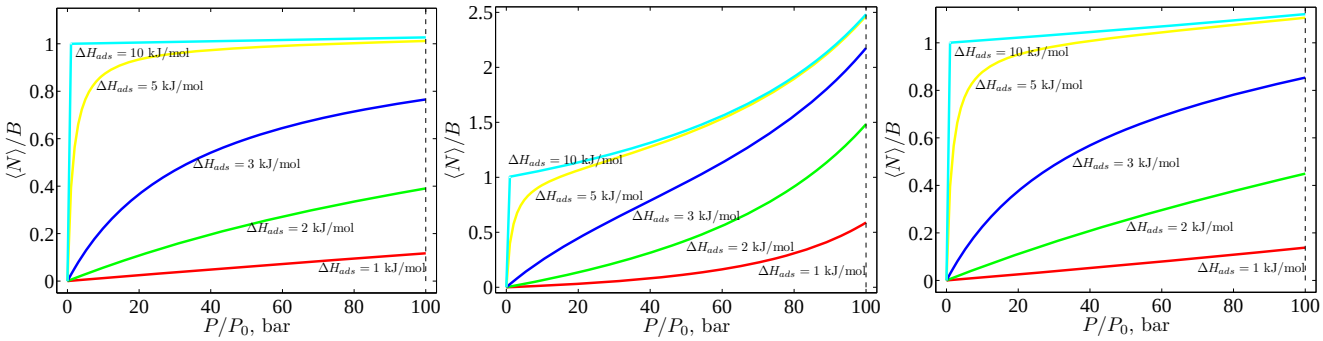

(a) $\Delta H^*_{ads} = 0\,\mathrm{kJ/mol}$ (b) $\Delta H^*_{ads} = 2\,\mathrm{kJ/mol}$ (c) Real case, $\Delta H^*_{ads} = 0.904\,\mathrm{kJ/mol}$

Figure 11: Isotherms for H_2 in the multilayer case for $T = 77$ K

Restricted Multilayer theory with molecular hydrogen. Now we analyze hydrogen through an application of RMT with n layers. For $\epsilon_2 = 0$ (or $\Delta H^*_{ads} = 0$), we obtain that $x = \alpha\frac{P}{P_0} \leq 2.6\times10^{-2}$. Moreover if $\Delta H_{ads} \leq 3\,\mathrm{kJ/mol}$, $cx = \exp\left(\frac{\Delta H_{ads}}{RT}\right)x \leq 2.83$ for T=77 K. That is why, in this case cx^n, has a small value for $n > 1$. But for $n = 1$ we have the monolayer case, which has already been considered. Further if we let $n \geq 2$, as $x \leq 2.6\cdot10^{-2}$ and $cx \leq 2.83$, we exclude from equation (14) all powers of x higher than the first power and obtain

$$\frac{\langle N\rangle}{B} = \frac{cx}{1+cx}\times\left(1+\frac{2x}{1+(c-2)x}\right).$$

This relation shows that the difference between monolayer theory and restricted multilayer is not very significant, if $\Delta H_{ads} \leq 3\,\mathrm{kJ/mol}$, because the multiplying factor is the sum of 1 and a function raised to the first power of x. Now we consider isotherms of hydrogen for different numbers of layers n, and different values of ΔH_{ads}, depending on the relative pressure P/P_0.

For small values of ΔH^*_{ads}, there is no significant dependence of $\langle N\rangle/B$ on the number of layers, whereas for high ΔH^*_{ads}, this dependency is noticeable.

C. Theory for the high temperature region

For the high temperature region (for instance, for $T = 298$ K), we should consider not only translational

part of the chemical potential for hydrogen, but also its rotational part (as the rotational activation temperature for hydrogen molecule is $T_r = 85.4$ K). The appropriate considerations (see section XII) show that considerations of the full chemical potential in our theory only alter α as follows (see eq. (17))

$$\alpha \to \alpha(2\,T_r)/T, \tag{17}$$

which for $T = 298$ K gives $\alpha = 5.1 \cdot 10^{-6}$ for full chemical potential. This can be compared with the value obtained at 77 K, $\alpha = 2.6 \cdot 10^{-4}$. Thus, all the equations from previous sections are valid for the high temperature region where the appropriate substitution of α is made.

VII. ISOTHERMS FOR DIFFERENT ΔH^*_{ads} IN RESTRICTED MULTILAYER CASE

Let us plot isotherms for values of ΔH^*_{ads} different from 0.904kJ/mol. Isotherms for $\Delta H^*_{ads} = 0$ and $\Delta H^*_{ads} = 0.5$ kJ/mol are similar (see Figure S13 and Figure S14) whereas the ones for $H^*_{ads} = 2$ kJ/mol (see Figure S15) are different due to the significant impact of higher levels.

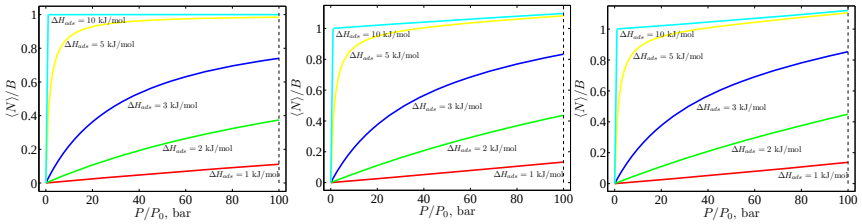

(a) T=77 K, $n = 1$ (b) T=77 K, $n = 2$ (c) T=77 K, $n = 5$

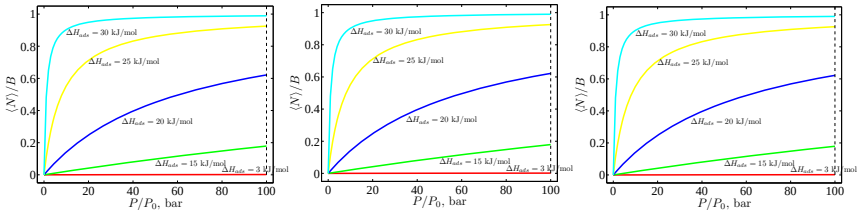

(d) T=298 K, $n = 1$ (e) T=298 K, $n = 2$ (f) T=298 K, $n = 5$

Figure 12: Isotherms for hydrogen in the restricted multilayer case when $\Delta H^*_{ads} = 0.904$ kJ/mol at T=77 K and T=298 K.

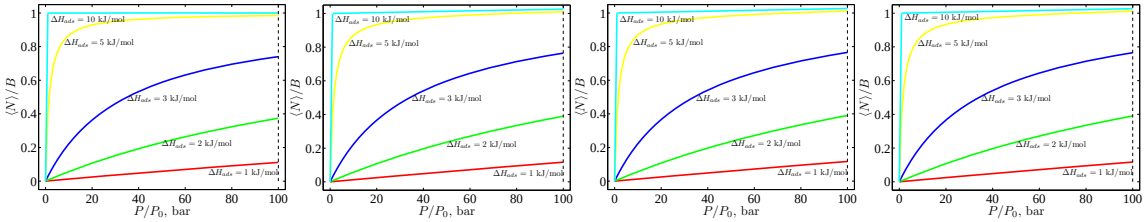

(a) $n = 1$ (b) $n = 2$ (c) $n = 5$ (d) $n = 10$

Figure 13: Isotherms for H_2 in restricted multilayer case ($n = 1$, 2, 5, 10) when $\Delta H^*_{ads} = 0$ kJ/mol for T=77 K.

A. Optimal parameters of the framework for the highest gas delivery using the Langmuir and BET theory

Enthalpy of adsorption ΔH_{ads}. We define

$$\beta_1 = \exp\{\Delta H_{ads}/(RT)\},\ \beta_2 = \exp\{\Delta H^*_{ads}/(RT)\},$$

$$\tilde{\beta_1} = \alpha\beta_1,\ \tilde{\beta_2} = \alpha\beta_2,$$

$$c = \beta_1/\beta_2,\ x = \alpha P/P_0\beta_2,$$

where α is a function of temperature that was defined previously. Deriving $\partial\Delta\nu/\partial\Delta H_{ads}$ for monolayer and multilayer theories gives the following values for optimal enthalpy ΔH^{opt}_{ads}.

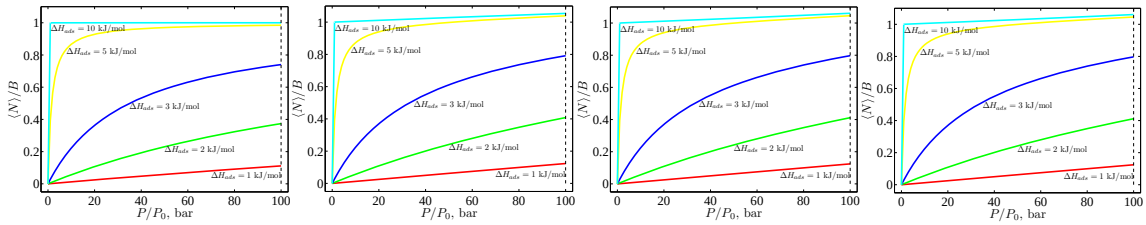

(a) $n = 1$ (b) $n = 2$ (c) $n = 5$ (d) $n = 10$

Figure 14: Isotherms for H_2 in restricted multilayer case (n = 1, 2, 5, 10) when $\Delta H^*_{ads} = 0.5$ kJ/mol for T=77 K.

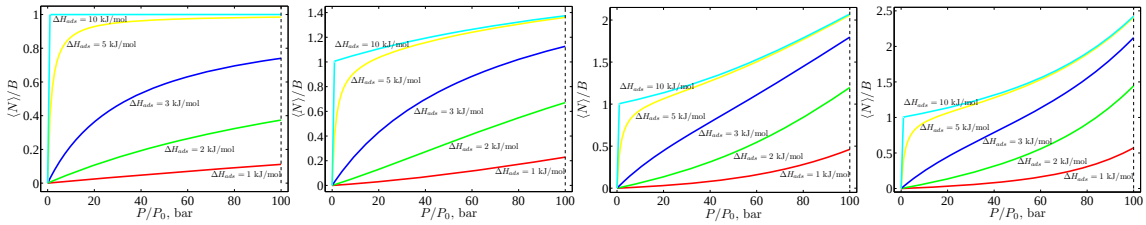

(a) $n = 1$ (b) $n = 2$ (c) $n = 5$ (d) $n = 10$

Figure 15: Isotherms for H_2 in restricted multilayer case (n = 1, 2, 5, 10) when $\Delta H^*_{ads} = 2$ kJ/mol for T=77 K.

For the **monolayer case**, we get the optimal value of adsorption enthalpy ΔH_{ads} as follows.

$$\Delta H^{opt}_{ads} = RT \ln \frac{1}{\alpha\sqrt{m}} = RT \ln \left(\frac{T^{5/2}}{\alpha_0 T_0^{5/2}} \sqrt{\frac{P_0}{P}} \right) \quad (18)$$

where $\alpha_0 = 2.6\, and \cdot 10^{-4}$, $T_0 = 77\, K$. For instance, for pressure P=100 bar and T=77 K we get $\Delta H_{ads} = 3.75$ kJ/mol.

To obtain the optimal enthalpy in the monolayer case for the high-temperature region (for instance, for T=298 K) we make the appropriate change of α (see eq. (17) in subsection VI C) and get

$$\Delta H^{opt}_{ads} = RT \ln \frac{1}{\alpha\sqrt{m}} = RT \ln \left(\frac{T^{7/2}}{\alpha_0 T_0^{7/2}} \sqrt{\frac{P_0}{P}} \right), \quad (19)$$

where $\alpha_0 = 5.1 \cdot 10^{-6}$ and $T_0 = 298$ K. Evaluating (19) for pressure P=100 bar and T=298 K, we get $\Delta H_{ads} =$ 24.5 kJ/mol.

To calculate $\Delta\nu$ in the **monolayer case** using the calculated optimal adsorption enthalpy, ΔH^{opt}_{ads}, we obtain,

$$\Delta\nu = \frac{\sqrt{m}-1}{\sqrt{m}+1}. \quad (20)$$

Substituting P=100 bar into (20), we get

$$\Delta\nu = 9/11 = 81.8\%.$$

The optimal adsorption enthalpy in **multilayer case** is given by eq. (21), given as

$$\Delta H^{opt}_{ads} = RT \ln \frac{1}{\alpha\sqrt{m}} + \beta_2 = RT \ln \left(\frac{T^{5/2}}{\alpha_0 T_0^{5/2}} \sqrt{\frac{P_0}{P}} + \exp \frac{\Delta H^*_{ads}}{RT} \right). \quad (21)$$

Comparing (18) and (21) indicates that as $T \to \infty$ (and even at relatively high temperature), there is nearly no difference in the optimal enthalpy of adsorption between the monolayer and multilayer cases. For instance, for P=100 bar and T=77 K, this difference is only 8 J/mol. But when $T \to 0$ in the monolayer case, $\Delta H^{opt}_{ads} \to 0$, whereas in the multilayer case, $\Delta H^{opt}_{ads} \to \Delta H^*_{ads}$.

To obtain the optimal enthalpy in the multilayer case for high-temperature region (for instance, for T=298 K), we make the appropriate change of α (see eq. (17)) and get

$$\Delta H^{opt}_{ads} = RT \ln \frac{1}{\alpha\sqrt{m}} + \beta_2 = RT \ln \left(\frac{T^{7/2}}{\alpha_0 T_0^{7/2}} \sqrt{\frac{P_0}{P}} + \exp \frac{\Delta H^*_{ads}}{RT} \right), \quad (22)$$

where $\alpha_0 = 5.1 \cdot 10^{-6}$, $T_0 = 298$ K.

To determine the difference in the factor ν between pressures P_0 and P, we get, in the multilayer case,

$$\Delta\nu = \frac{1+\alpha\beta_2\sqrt{m}}{1+\sqrt{m}} \left[\frac{\sqrt{m}}{1-\alpha m\beta_2} - \frac{1}{1-\alpha\beta_2} \right]. \quad (23)$$

As the assumption of an infinite number of layers is not realistic, from (23), we obtain a restriction on the range of pressures. This theory works if

$$m < \frac{1}{\alpha\beta_2}. \tag{24}$$

For T=298 K, the upper border according to (24) equals 137,200 bar, which is far more than the value of 100 bar considered previously. For T=77 K, the upper bound is also far more than that of 100 bar, and equals 955 bar.

For molecular hydrogen, ΔH^*_{ads} is relatively low. The graph in Figure 5 is the same for all three cases, depicting monolayer, multilayer and restricted multilayer cases for any number of layers. Discrepancies are significant only at very low temperatures. From equations (18), (21) and (6) we determine that optimal enthalpy increases with temperature.

We plot in color the dependence of the optimal enthalpy on temperature, T, and pressure, P, in all three cases for low and high temperatures: monolayer (see Figure 16a, d), multilayer (see Figure 16b, e) and restricted multilayer for 3 layers (see Figure 16c, f).

I the multilayer case there is a restriction from equation (24) on the possible value of pressure. This restriction works only when the temperature is relatively low (the bound P=100 bar is reached at 45.5 K); for higher temperatures all the pressures up to 100 bar are allowed by the restriction.

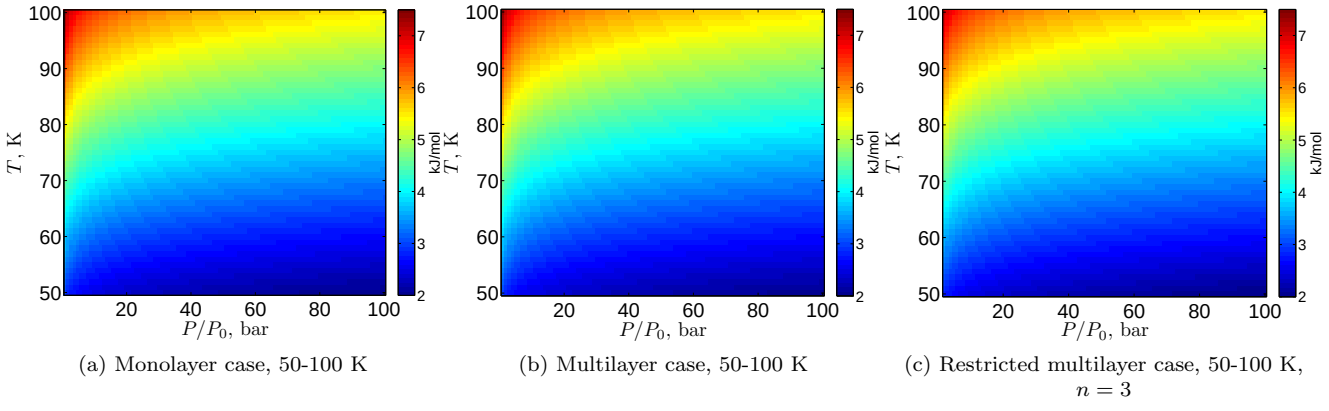

(a) Monolayer case, 50-100 K (b) Multilayer case, 50-100 K (c) Restricted multilayer case, 50-100 K, $n = 3$

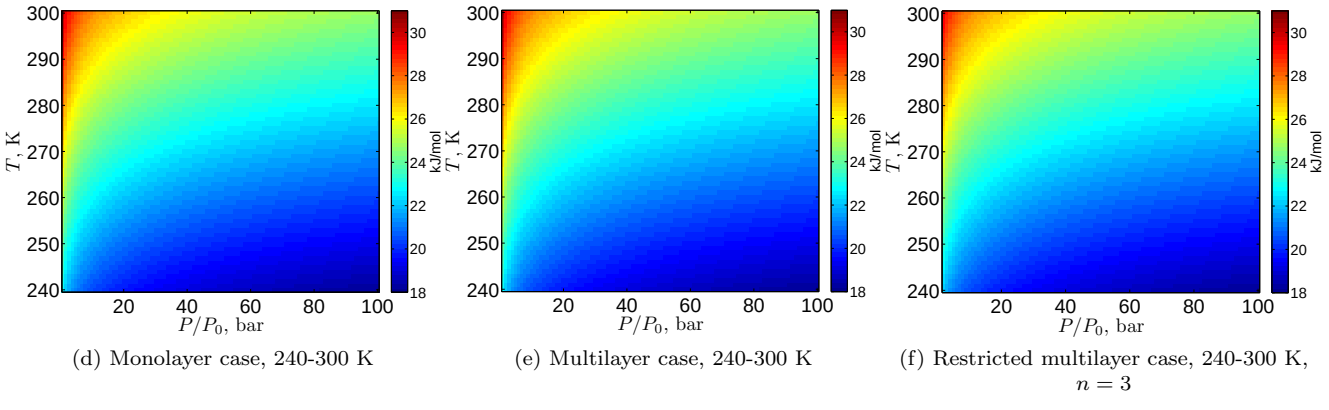

(d) Monolayer case, 240-300 K (e) Multilayer case, 240-300 K (f) Restricted multilayer case, 240-300 K, $n = 3$

Figure 16: Temperature and pressure dependence of optimal enthalpy ΔH^{opt}_{ads} for low and high temperature region

VIII. CUBIC FRAMEWORK WITH INTERPENETRATION.

Another framework explored in this work is one where there is interpenetration present, where frameworks of the same kind are catenated starting with a two-fold degree and eventually reaching a maximum limited by the space inside the pores.

We consider the framework of q interpenetrated cubic nets with linkers that are cylinders of length l and base radii r, and SBU-nodes that we treat as spheres with diameter d. If the volume of the porous material is V, then we get

$$\frac{V}{(d+l)^3}$$

cells and therefore the uptake in number of hydrogen molecules would be

$$N = \frac{V}{(d+l)^3} B \frac{N}{B}(\tilde{n}),$$

where $\tilde{n}$ is an effective number of layers, B is a number of sites and $\frac{N}{B}(\tilde{n})$ is $\frac{N}{B}$ for restricted multilayer case with $\tilde{n}$ layers. In order to estimate the effective number of layers one can consider the longest distance in a cubic cell, which is its main diagonal, and thus get the effective number of layers in the following equation,

$$\tilde{n} = \frac{\sqrt{3}(d+l)}{D+\delta},$$

where, D is the diameter of a hydrogen molecule and δ is the characteristic distance between them. Another approach takes into account the symmetry of adsorption in a cubic cell and therefore the effective number of layers is smaller. In this approach the effective longest distance is not the diagonal but is instead the edge of a cube. Therefore, we get

$$\tilde{n} = \frac{d+l}{D+\delta}. \tag{25}$$

Thus we use eq. (25) for estimating the effective number of layers. We should also note that if eq. (25) gives fractional number of layers e.g. 1.54, one can pick up either 1 or 2 layers. In this article we use the biggest integer number not higher than $\tilde{n}$.

Let us consider the case of cubic frameworks with an interpenetration of degree q. In this case, the length of the linker is l, the diameter of the SBU-node, which is considered to be a sphere, is d, and the radius of the linker is r. The factor γ, which, in this case, defines the share of the free volume, equals

$$\gamma = 1 - q\frac{\pi/6d^3 + 3\pi r^2 l}{(d+l)^3}.$$

The surface area of a pore is equal to

$$S_p = 6(d+l)^2 - 6\pi d^2/4 = 6\left[(d+l)^2 - \pi d^2/4\right].$$

The optimal values of ΔH_{ads} are very close: 4.47 kJ/mol and 4.43 kJ/mol, respectively. Isotherms with these enthalpies of adsorption are plotted on the Fig-

B. MOF-177

We assume that it is caused by the slight decrease of adsorption enthalpy reported in [9] which can also be supported by the fact that excess uptake in region of high

The optimal values of ΔH_{ads} are very close: 4.07 kJ/mol and 4.05 kJ/mol, respectively. Isotherms for these enthalpies of adsorption are displayed in Fig-

X. EFFECTIVE RADIUS OF HYDROGEN

Now we calculate the effective radius of hydrogen necessary for the number of sites calculations. Let the rela-

Given that the degree of interpenetration is q, we can say that

$$S = qS_p,$$

and therefore

$$B = \frac{qS_p}{\pi r_{\mathrm{H_2}}^2}.$$

Now let us apply this equation to determining the adsorption in MOF-9, which is a cubic interpenetrated framework of degree two. For this MOF, $d = 9.65\,\text{Å}$, $l = 11.88\,\text{Å}$ and $2r = 5\,\text{Å}$. Thus we get

$$\gamma = 1 - 2 \cdot 0.119 = 0.762.$$

This agrees well with experimental measurements of $\gamma = 0.71$ that were carried out by Eddaoudi et al. [8]. According to (26), $S_p = 2340\ \text{Å}^2$, and therefore the number of sorption sites is $B = 194.16 \approx 194$, and the number of layers is $\tilde{n} = 3.9 \approx 4$. The uptake (2) gives

$$m = 45.9\frac{N}{B}(4)\ \text{g/L}.$$

IX. COMPARISON TO EXPERIMENTS

A. MOF-5

We assume that the discrepancy in the low-pressure region can also be caused a by slight decrease of the adsorption enthalpy reported in [9]. This assumption is further supported by the fact that excess uptake in the region of high pressures and low temperatures is mainly sensitive not to changes in adsorption enthalpy, but to changes in pore properties [10]. We will use two optimized measures. The first is the sum of squares of deviations of uptake. The second is the sum of the absolute values of deviations. The dependency of these measures on enthalpy of adsorption can be seen in Figure S17a and Figure S17b. ure S18 a and Figure S18 b. The square root of the average square deviation and absolute deviation are, respectively, 0.81 (g/L) and 0.65 g/L.

pressures and low temperatures is mainly sensitive not to changes in adsorption enthalpy, but to changes in pore properties [10]. We will use two optimized enthalpy estimations. The first one is sum of squares of deviations of uptake. The second is the sum of absolute values of deviations. The dependency of this measures on enthalpy of adsorption can be seen in Figure S19 a and Figure S19b. ure S20a and Figure S20b. The square root of the average square deviation and the absolute deviation are, respectively, 0.64 (g/L) and 0.51 g/L.

tion between the number of available sites and the surface area be

$$B = \theta_0 S.$$

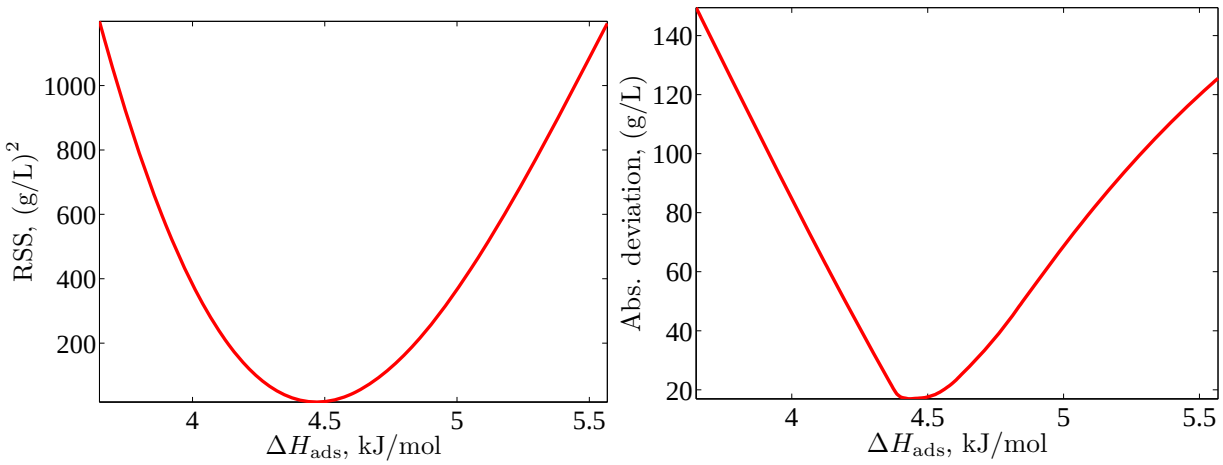

(a) Sum squares of deviations

(b) Sum absolute values of deviations

Figure 17: Two measures of fit for MOF-5

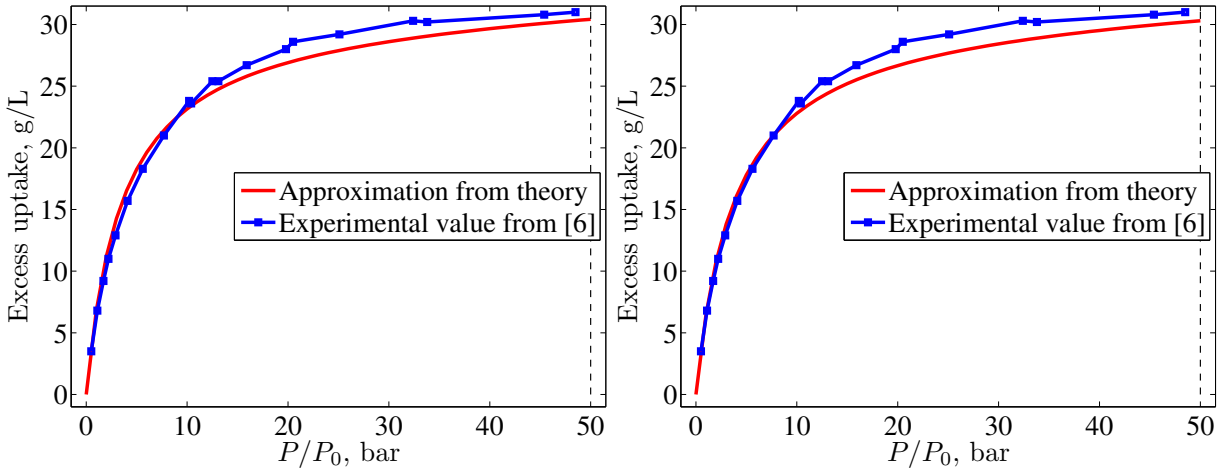

(a) $\Delta H_{ads} = 4.470$ kJ/mol

(b) $\Delta H_{ads} = 4.431$ kJ/mol

Figure 18: Isotherm for MOF-5 for two obtained optimal enthalpies ΔH^*_{ads}

A. T=77 K

To obtain the coefficient we use the data from [9],

$$N = \frac{S}{S_0} = B\frac{N}{B}(\tilde{n}) = \theta_0 S\frac{N}{B}(\tilde{n}),$$

where S_0 is the characteristic surface area occupied by one adsorbed molecule of hydrogen and S is a surface area. We will make the assumption that

$$\frac{N}{B}(\tilde{n})$$

does not depend on MOF, which is based on the insignificant impact of slight changes in the enthalpy of adsorption at such a low temperature. The other way to count

Table IV: Surface area and excess uptake for different MOFs

Surface area, m^2/g	Uptake, mg/g	MOF
1100	22	MOF-74
2300	34	HKUST-1
2400	37	IRMOF-11
3300	50	IRMOF-6
4200	53	IRMOF-1
4700	68	IRMOF-20
5700	75	MOF-177

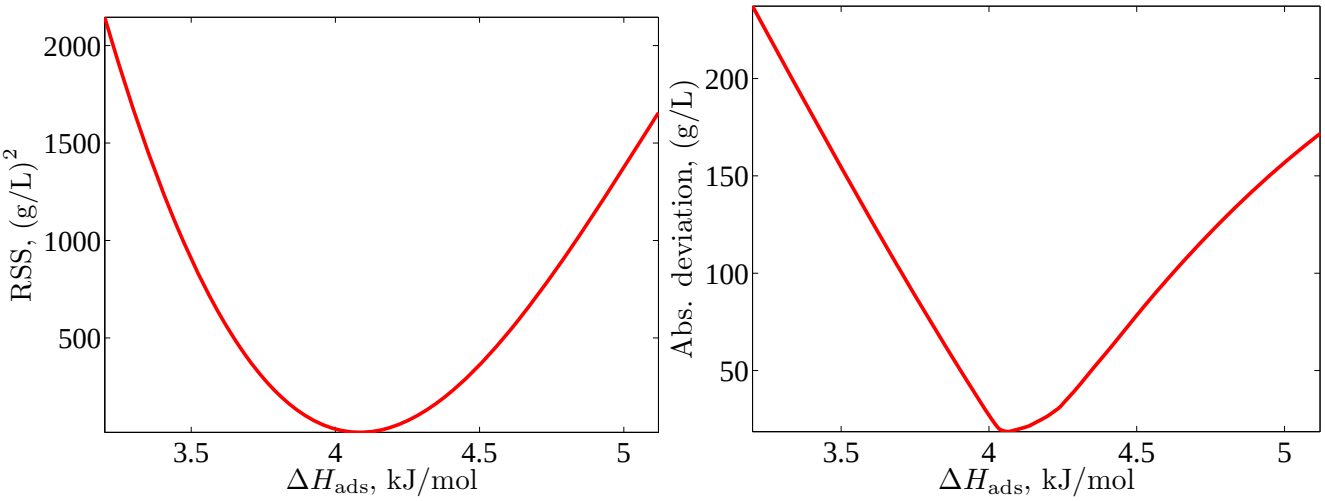

(a) Sum squares of deviations

(b) Sum absolute values of deviations

Figure 19: Two measures of fit for MOF-177

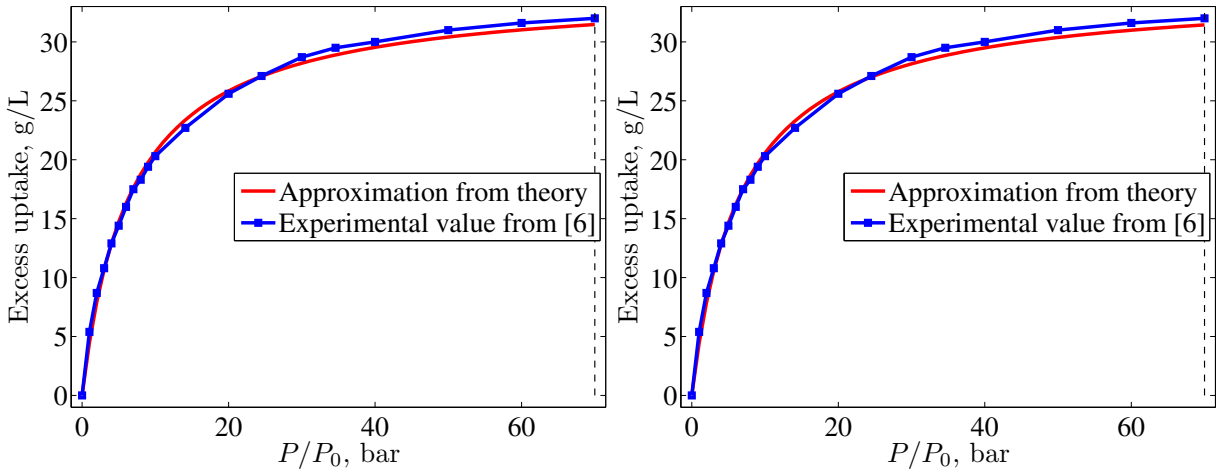

(a) $\Delta H_{ads} = 4.067$ kJ/mol

(b) $\Delta H_{ads} = 4.054$ kJ/mol

Figure 20: Isotherm for MOF-177 for two obtained optimal enthalpies ΔH^*_{ads}

the excess uptake is as follows,

$$\theta = \frac{m}{S} = \frac{N\mu}{N_A S} = \frac{2}{N_A S_0}\text{g/m}^2.$$

When fitting a linear model for data from table SV, we obtain

$$\theta = 0.0139\text{mg/m}^2.$$

Therefore, we get

$$S_0 = 10^{20}\text{Å}^2 \frac{2\,\text{g/mol}}{0.0139 \cdot 10^{-3}\text{g}\, 6.02 \cdot 10^{23}\text{mol}^{-1}} = 23.9\,\text{Å}^2.$$

And thus the effective radius of hydrogen equals

$$r_{H_2} = \sqrt{\frac{S_0}{\pi}} = 2.76\,\text{Å}.$$

B. T=298 K

To obtain the coefficient we use the data from [18],

$$N = \frac{S}{S_0} = B\frac{N}{B}(\tilde{n}) = \theta_0 S\frac{N}{B}(\tilde{n}),$$

where S_0 is characteristic surface area occupied by one adsorbed molecule of hydrogen and S is a surface area.

Table V: Surface area and excess uptake for different Li-MOFs

Surface area, m^2/g	Uptake, mg/g	MOF
3047	50.86	IRMOF-1-4Li
3620	58.97	IRMOF-8-6Li
4135	72.77	MOF-177-15Li
5558	87.34	MOF-200-27Li

We will make the assumption that

$$\frac{N}{B}(\tilde{n})$$

does not depend on MOF because, at such a pressure and such a high enthalpy of adsorption, the saturation of the first layer is nearly reached, whereas the second and subsequent layers are not as attracted to one another, since $\Delta H^*_{ads} < RT$. The other way to count the excess uptake is the following

$$\theta = \frac{m}{S} = \frac{N\mu}{N_A S} = \frac{2}{N_A S_0}\mathrm{g/m^2}.$$

After fitting a linear model for the data from table SV, we obtain

$$\theta = 0.0164\mathrm{mg/m^2}.$$

Therefore we get

$$S_0 = 10^{20}\mathrm{\AA}^2 \frac{2\,\mathrm{g/mol}}{0.0139\cdot 10^{-3}\mathrm{g}\, 6.02\cdot 10^{23}\mathrm{mol}^{-1}} = 20.3\,\mathrm{\AA}^2.$$

And thus the effective radius of hydrogen equals

$$r_{H_2} = \sqrt{\frac{S_0}{\pi}} = 2.54\,\mathrm{\AA}.$$

We will also use this effective radius of hydrogen for temperatures which are close to 298 K, for 243 and 273 K.

XI. CHEMICAL POTENTIAL FOR HIGH TEMPERATURES

For low temperatures (e.g., for 77 K), rotations in hydrogen are not significant, because the rotation activation temperature is 85.4 K and therefore we only used the translational part of chemical potential. Here we derive the rotational chemical potential for high temperatures. Consideration of both high temperature and low temperature cases can be found in [19]. As the vibration activation temperature is 6100 K, we do not consider the vibrational part of chemical potential.

Due to nuclear symmetry, the normal term of a hydrogen molecule has different degree of degeneration for rotational levels with odd and even orbital moment K. The molecules with an even total spin ($S = 0$ for hydrogen) must have an even orbital moment (0, 2,...), whereas molecules with an odd total spin ($S = 1$ for hydrogen) must have an odd orbital moment (1, 3,...). The energy corresponding to the orbital movement with moment K is

$$\frac{\hbar^2 K(K+1)}{2I},$$

where $I = m/2\, r_0^2$, where m is a mass of hydrogen atom and r_0 is the equilibrium distance between atoms in molecule. We introduce the designation

$$k_B T_r = \hbar^2/2I,$$

where T_r is the rotation activation temperature. For hydrogen $T_r = 85.4$ K. Further hydrogen modification with odd spin is called ortho- or u-hydrogen, whereas hydrogen modification with even spin is called para- or g-hydrogen. Relative degenerations of these two modifications are $g_u = 3/4$ and $g_g = 1/4$, respectively. Thus the partition functions for the modifications are

$$Z_u = \sum_{K=1,\,3,\ldots} (2K+1)\exp(-T_r/TK(K+1)), \quad (26)$$

and

$$Z_g = \sum_{K=0,\,2,\ldots} (2K+1)\exp(-T_r/TK(K+1)). \quad (27)$$

Therefore the full partition function is

$$Z = g_u Z_u + g_g Z_g = \frac{Z_g + 3Z_u}{4}. \quad (28)$$

For high temperatures,

$$Z_u \approx Z_g \approx 1/2 \sum_{K=0,\,1,\,2,\ldots} (2K+1)\exp(-T_r/TK(K+1))$$

which we approximate by an integral

$$\sum_{K=0,\,1,\,2,\ldots} (2K+1)\exp(-T_r/TK(K+1)) \approx \sum_{K=0,\,1,\,2,\ldots} 2K\exp(-T_r/TK^2) \approx \int_0^\infty \exp(-T_r/TK^2)dK^2 = T/T_r.$$

Thus $Z \approx T/(2\,T_r)$ and the corresponding free energy

$$F_{rot} = -NkT\log\frac{T}{2\,T_r}.$$

Finally we get the equation for rotational part of chemical

potential for high temperatures

$$\mu_{rot} = -kT \log \frac{T}{2\,T_r}. \quad (29)$$

XII. THEORY WHEN CONSIDERING FULL CHEMICAL POTENTIAL

In this section we show how it is necessary to alter the calculations which were previously presented for the translational part of chemical potential in order to consider the rotational part of the chemical potential. We use $\lambda = \exp(\mu/RT)$.

$$\lambda = \exp(\mu/kT) = \exp(\mu_{tr}/kT) \times \exp(\mu_{rot}/kT) = \alpha P/P_0 \exp(\mu_{rot}/kT), \quad (30)$$

where μ_{tr} and μ_{rot} are the translational and rotational parts of chemical potential, respectively. As the enthalpy of adsorption is relatively high, we can still consider adsorption as localized. Therefore, from eq. (30) and eq. (29), we get

$$\lambda = \alpha \frac{2T_r}{T} P/P_0. \quad (31)$$

From equation (31), we obtain that the consideration of full chemical potential results only in an appropriate change of α

$$\alpha_{new} = \alpha \frac{2T_r}{T}. \quad (32)$$

XIII. DEPENDENCE OF ENTHALPY OF ADSORPTION ON PRESSURE

For Li-metalated frameworks with high enthalpy of adsorption that face high uptake at room temperature, there is a significant dependence of the enthalpy of adsorption on uptake and therefore on pressure. Here we illustrate how this dependence was calculated for MOF-200-27Li at room temperature. At the end of this section we provide tables for calculated enthalpies for MOF200-27Li and MOF-177-15Li at 243, 273 and 298 K.

From [18], we get the dependence of adsorption enthalpy on total weight uptake, for which we use the following linear approximation

$$\Delta H_{ads} = Q_{st} = (29 - u)\,\mathrm{kJ/mol},$$

where u is the weight total uptake in units of percent. As $\Delta H^*_{ads} \ll RT \ll \Delta H_{ads}$, we use monolayer theory. We also make an assumption that reaching 10% of total uptake is nearly the same as total uptake at saturation. We also apply our theoretical approximation of excess uptake to total uptake, and therefore we obtain

$$u = \frac{10}{1 + 1/\alpha \cdot P_0/P \exp(-\Delta H_{ads}/RT)}.$$

Thus we get the following equation

$$29 - \Delta H_{ads}/1000 = \frac{10}{1 + 1/\alpha \cdot P_0/P \exp(-\Delta H_{ads}/RT)}. \quad (33)$$

For $T = 298$ K, equation (33) gives

$$29 - 2.4764\,x = \frac{10}{1 + 1.954 \cdot 10^5/m \cdot e^{-x}},$$

where $x = \Delta H_{ads}/RT$ and $m = P/P_0$. Solving the last equation at different pressures P, we obtain the data for enthalpy at $T = 298$ K at different pressures (see tab. VI). Using the same approach we obtain the enthalpies for other temperatures.

Table VI: Enthalpy of adsorption of MOF-200-27Li for different pressures for T=243, 273 and 298 K

P, bar	$\Delta H_{ads}/RT$ for T=298 K	$\Delta H_{ads}/RT$ for T=273 K	$\Delta H_{ads}/RT$ for T=243 K
1	10.8607	11.2894	11.7611
5	10.1310	10.4301	10.8103
10	9.7863	10.0511	10.4133
20	9.4388	9.6790	10.0346
30	9.2383	9.4681	9.8251
40	9.0988	9.3228	9.6831
50	8.9927	9.2131	9.5774
60	8.9078	9.1258	9.4942
70	8.8372	9.0536	9.4261
80	8.7772	8.9925	9.3690
90	8.7252	8.9397	9.3201
100	8.6795	8.8934	9.2776

Table VII: Enthalpy of adsorption of MOF-177-15Li for different pressures for T=243, 273 and 298 K

P, bar	$\Delta H_{ads}/RT$ for T=298 K	$\Delta H_{ads}/RT$ for T=273 K	$\Delta H_{ads}/RT$ for T=243 K
1	10.4573	10.9922	11.5831
5	9.9044	10.2709	10.7403
10	9.6198	9.9404	10.3879
20	9.3265	9.6143	10.0561
30	9.1562	9.4303	9.8760
40	9.0378	9.3044	9.7560
50	8.9481	9.2100	9.6680
60	8.8765	9.1354	9.5997
70	8.8174	9.0742	9.5445
80	8.7674	9.0227	9.4988
90	8.7242	8.9785	9.4601
100	8.6864	8.9400	9.4268